



Temperature enhanced succinate production concurrent with increased central metabolism turnover in the cyanobacterium *Synechocystis* sp. PCC 6803

Hasunuma, Tomohisa

Matsuda, Mami

Kato, Yuichi

John Vavricka, Christopher

Kondo, Akihiko

(Citation)

Metabolic Engineering, 48:109-120

(Issue Date)

2018-07

(Resource Type)

journal article

(Version)

Accepted Manuscript

(Rights)

© 2018 Elsevier B.V.

This manuscript version is made available under the CC-BY-NC-ND 4.0 license

<http://creativecommons.org/licenses/by-nc-nd/4.0/>

(URL)

<https://hdl.handle.net/20.500.14094/90004904>



1 **Temperature enhanced succinate production concurrent with**
2 **increased central metabolism turnover in the cyanobacterium**
3 ***Synechocystis* sp. PCC 6803**

4

5 Tomohisa Hasunuma^{a*}, Mami Matsuda^a, Yuichi Kato^a, Christopher John Vavricka^a
6 and Akihiko Kondo^{a,b}

7

8

9 ^a Graduate School of Science, Innovation and Technology, Kobe University, 1-1
10 Rokkodai, Nada, Kobe 657-8501, Japan

11 ^b Biomass Engineering Program, RIKEN, 1-7-22 Suehiro, Tsurumi, Yokohama,
12 Kanagawa 230-0045, Japan

13

14

15

16 *Corresponding author: Tomohisa Hasunuma

17 Graduate School of Science, Technology and Innovation, Kobe University, 1-1
18 Rokkodai, Nada, Kobe 657-8501, Japan

19 Tel: +81-78-803-6356; Fax: +81-78-803-6192

20 E-mail: hasunuma@port.kobe-u.ac.jp

21

22

23

24 **ABSTRACT**

25 Succinate is a versatile petrochemical compound that can be produced by
26 microorganisms, often from carbohydrate based carbon sources. Phototrophic
27 cyanobacteria including *Synechocystis* sp. PCC 6803 can more efficiently produce
28 organic acids such as succinate without sugar supplementation, via photosynthetic
29 production of glycogen followed by glycogen utilization, typically under dark
30 conditions. In this study, *Synechocystis* 6803 bioproduction of organic acids under
31 dark anoxic conditions was found to increase with elevation of temperature from
32 30°C to 37°C. The further enhancement of succinate bioproduction by
33 overexpression of the rate limiting enzyme phosphoenolpyruvate carboxylase
34 resulted in improved glycogen utilization. To gain more insight into the
35 mechanisms underlying the increased organic acid output, a novel temperature
36 dependent metabolomics analysis was performed. Adenylate energy charge was
37 found to decrease along with elevating temperature, while central metabolites
38 glucose 6-phosphate, fructose 6-phosphate, fructose 1,6-bisphosphate, glycerol 3-
39 phosphate, malate, fumarate and succinate increased. Temperature dependent ¹³C-
40 labeling metabolomics analysis further revealed a glycolysis to TCA bottleneck,
41 which could be overcome by addition of CO₂, leading to even higher organic acid
42 production. Optimization of initial cell concentration to 25 g-dry cell weight/L, in
43 combination with 100 mM NaHCO₃ supplementation, afforded a succinate titer of
44 more than 1.8 g/L, the highest reported autotrophic succinate titer. Succinate titers
45 remained high after additional knockout of *ackA*, resulting in the highest reported
46 autotrophic D-lactate titer as well. The optimization of *Synechocystis* 6803 organic

47 acid production therefore holds significant promise for CO₂ capture and utilization.

48

49

50 **Key words:**

51 Autofermentation; Cyanobacteria; Lactate; Metabolomics; Succinate; *Synechocystis*;

52 Temperature

53

54 **1. Introduction**

55 The rapid development of the petrochemical industry in the 20th century has
56 created a mass consumption and disposal social structure, leading to the over-
57 generation of greenhouse gasses including carbon dioxide (CO₂) and global climate
58 change. In order to address these problems and help build a sustainable low-
59 carbon future society, it is necessary to develop technologies to biologically
60 produce fuels and commodity chemicals from renewable biomass. Recently, non-
61 food-based lignocellulosic biomass that exists abundantly on land has attracted
62 attention as a renewable feedstock for microbial fermentation to produce a wide
63 variety of chemicals. However, recalcitrant structures of lignocellulosic biomass
64 make it difficult to generate fermentable sugars from component cellulose and
65 hemicellulose with high yield.

66 Photosynthetic algae directly convert CO₂ to useful substances including
67 lipid, starch, glycogen, pigments and organic acids ([Aikawa et al., 2013](#); [Dismukes](#)
68 [et al., 2008](#); [Hasunuma et al., 2016](#), [Ho et al., 2017](#); [Wijffels et al., 2013](#)), which can
69 be utilized to avoid the use of more expensive sugars as well as complicated plant-
70 biomass decomposition processes. Furthermore, algae cultivation does not require
71 agricultural resources such as farmland or fresh water ([Iijima et al., 2015](#)).

72 The unicellular cyanobacterium *Synechocystis* sp. PCC 6803 (hereafter
73 *Synechocystis* 6803) is the first algae to be genome decoded ([Kaneko et al., 1996](#)).
74 Along with the development of genetic engineering tools, *Synechocystis* 6803
75 metabolic pathways have been successfully modified to enhance photosynthetic
76 activity and to produce alcohols, diols, hydrocarbons, organic acids and other

77 valuable chemicals (Angermayr et al., 2015; Formighieri et al., 2015; Hasunuma et
78 al., 2014; Lai and Lan 2015; Lan and Wei, 2016; Wang et al., 2016).

79 *Synechocystis* 6803 inherently produces organic acids including D-lactate
80 and succinate by catabolism of the primary storage polysaccharide glycogen, which
81 accumulates during photosynthesis (Hasunuma et al., 2016). As carbon sources
82 such as sugars and glycerol are not necessary, this type of catabolism is referred to
83 as autofermentation (McNeely et al., 2010). Lactate typically serves as a building
84 block for the synthesis of a bio-based plastic, polylactic acid (PLA). Notably,
85 stereocomplex-type PLA composed of L- and D-lactate is promising due to a high
86 melting point (ca. 230°C) (Ikeda et al., 1987). The current industrial biological
87 production of D-lactate (Wee et al., 2006) remains to be established and is
88 therefore considered to be more important than that of L-lactate.

89 Succinate is also an important raw material of poly(butylene succinate),
90 polyurethanes and other green sustainable plastics (Choi et al., 2015; Delhomme et
91 al., 2009). Various chemicals produced in the current petrochemical industry
92 including adipic acid, 1,4-butanediol, γ -butyrolactone, *N*-methylpyrrolidone and
93 tetrahydrofuran can be produced from succinate as well (Akhtar et al., 2014).

94 The metabolic pathways of autofermenting cyanobacteria are not well
95 characterized as of yet. Recently, dynamic metabolomics using ¹³C labeling has
96 clarified that succinate is biosynthesized from glycogen via glycolysis, the
97 anaplerotic pathway and reductive TCA cycle in *Synechocystis* 6803 under dark
98 anoxic conditions (Hasunuma et al., 2016). However, optimal culture environments
99 to maximize production of succinate have not yet been determined.

100 Temperature is an important control element in the fermentation process
101 to efficiently produce target molecules (Gourdon and Lindley, 1999; Shin et al.,
102 2007). Yet, the influence of temperature regulation on the total metabolic system of
103 a microorganism has not been reported to our knowledge (Yurkovich et al., 2017).

104 The optimal growth temperature of *Synechocystis* 6803 is 30-32°C (Tasaka
105 et al., 1996). In the present study of *Synechocystis* 6803, elevated temperatures
106 were found to increase production of organic acids including D-lactate and
107 succinate. The highest production of D-lactate and succinate was observed at 37°C
108 to 40°C.

109 So far, the optimal temperature range of various enzymes involved in
110 central metabolism has been investigated *in vitro*. However, *in vivo* metabolic
111 turnover, which is dependent on activated-enzyme level and intracellular
112 environment such as molecular crowding, differs from the *in vitro* data. Thus, in the
113 present study, influence of elevated temperature on central metabolism was
114 systematically analyzed using a dynamic metabolome analysis developed by
115 combining *in vivo* ¹³C labeling, metabolomics and mass distribution determination.
116 This comprehensive approach afforded direct observation of *in vivo* kinetics and
117 carbon distribution in *Synechocystis* 6803. Elevating temperature to 37°C was
118 found to enhance organic acid bioproduction in both wild type and
119 phosphoenolpyruvate carboxylase (PEPC) overexpressing *Synechocystis* 6803.
120 Furthermore, a glycolysis to TCA bottleneck was discovered and alleviated via
121 addition of CO₂, which significantly increased succinate titers to 1,802 mg/L.

122

123 **2. Materials and Methods**

124 **2.1. Strains and culture conditions**

125 A recombinant *Synechocystis* 6803 strain, referred to as Ppc-ox, overexpresses the
126 endogenous PEPC gene (*ppc*, *sll0920*) under the control of the *trc* promoter. The
127 Ppc-ox strain was constructed from a wild type GT strain (Williams, 1988) as
128 described previously (Hasunuma et al., 2016). Recombinant and GT strains were
129 cultivated in BG11 medium (Rippka et al., 1979) with and without 50 mg/L
130 kanamycin, respectively, under photoautotrophic conditions. Cell density was
131 observed by optical density at 750 nm (OD₇₅₀). Sampling volumes were determined
132 based on g-dry cell weight (DCW). DCW was measured after harvesting cells by
133 filtration, washing with 20 mM ammonium bicarbonate, and lyophilization.

134

135 **2.2 Construction of a recombinant strain**

136 The Ppc-ox strain was transformed with pTCP1299 (Osanai et al., 2015) using a
137 previously described method (Hasunuma et al., 2016) to yield strain Ppc-ox/ Δ *ackA*.
138 Colonies resistant to 50 mg/L kanamycin and 34 mg/L chloramphenicol were
139 selected. Knockout of *ackA* (*sll1299*) was confirmed by PCR using the specific
140 primers 5'-TCAGCATTGATACCACTATGGGCTTCAC-3' and 5'-
141 GACAGCCCAGAGACTCCGAGCAAACCGGA-3'.

142

143 **2.3 Batch fermentation under anaerobic conditions**

144 After pre-cultivation in BG11 medium, cells were inoculated into modified-BG11
145 medium containing 50 mM Hepes-KOH (pH 7.8) and 5 mM NH₄Cl as a nitrogen

146 source instead of NaNO₃ at a biomass concentration of 0.1 g-DCW/L.
147 Photoautotrophic cultivation proceeded for 3 days under 1% (v/v) CO₂ and
148 continuous light irradiation of 105-115 μmol photons/m²/s at 30°C as described
149 previously (Hasunuma et al., 2016). After photoautotrophic cultivation, cells were
150 transferred into 100 mM Hepes-KOH (pH 7.8) at biomass concentrations of 5-50 g-
151 DCW/L and cultivated at 30-40°C under anaerobic conditions as described
152 (Hasunuma et al., 2016). Organic acids secreted into fermentation medium were
153 analyzed with high-performance liquid chromatography (HPLC), while minor
154 components were quantified with capillary electrophoresis-mass spectrometry
155 (CE-MS) (CE, Agilent G7100; MS, Agilent G6224AA LC/MSD TOF; Agilent
156 Technologies, Palo Alto, CA, USA) again as described (Hasunuma et al., 2016).

157

158 **2.4 Analysis of intracellular metabolites**

159 Cells (5 mg DCW) were collected by filtration with 1-μm pore size PTFE disks
160 (Omnipore; Millipore, Billerica, MA,). After washing with 20 mM ammonium
161 carbonate at 4°C, intracellular metabolites were extracted according to previous
162 methods (Hasunuma et al., 2016). To remove solubilized protein, the extract was
163 filtered through a 3 kDa cut-off membrane (Millipore). The metabolites were
164 analyzed using a CE-MS system as described above. Intracellular glycogen was
165 determined with HPLC after extraction from cells and enzymatic hydrolysis
166 (Hasunuma et al., 2016).

167

168 **2.5 ¹³C-labeling metabolomics**

169 Metabolite turnover in *Synechocystis* 6803 was determined by the combination of
170 *in vivo* ¹³C-labeling and CE-MS analysis (Hasunuma et al., 2016). Cells were labeled
171 in 100 mM Hepes-KOH (pH 7.8) containing 2 g/L [U-¹³C] glucose for 0.5-3 h. After
172 cell collection and metabolite extraction, mass spectra of the intracellular
173 metabolites were analyzed using CE-MS to observe mass shifts from ¹²C to ¹³C in
174 metabolites. ¹³C fractions, ratios of ¹³C to total carbon, were calculated by relative
175 isotopomer abundance (m_i) of metabolites incorporating i ¹³C atoms as follows:

$$176 \quad m_i(\%) = \frac{M_i}{\sum_{j=0}^n M_j} \times 100$$

$$177 \quad {}^{13}\text{C fraction}(\%) = \sum_{i=1}^n \frac{i \times m_i}{n}$$

178 where M_i represents the isotopomer abundance of metabolite incorporating i ¹³C
179 atoms, and n is the number carbon atoms in the metabolite.

180

181 **2.6 Enzyme assay**

182 Enzyme assays were performed using cells cultivated for 24 h under dark anoxic
183 condition as described in **Section 2.3**. Activities of PEPC were measured as
184 described previously (Hasunuma et al., 2016). NAD-dependent malate
185 dehydrogenase (MDH) activity was determined as follows. About 50 mg-DCW of
186 cells were collected by centrifugation at 6,000 x g for 10 min at 4°C. After
187 discarding the supernatant and washing with extraction buffer (18 mM KH₂PO₄, 27
188 mM Na₂HPO₄, 15 mM MgCl₂, and 100 μM EDTA, pH 8.0), cells were disrupted in 3
189 mL of the extraction buffer by sonication. Cell debris was removed by

190 centrifugation at 20,000 x g for 20 min at 4°C to obtain protein extract as
191 supernatant. MDH assay was performed in 1.5 mL aliquots containing 50 mM Tris-
192 HCl (pH7.5), 200 µM NADH, 0.5 mM oxaloacetate and 250 µL of protein extract.
193 Replicate aliquots without oxaloacetate were used as controls. MDH activity was
194 determined by measuring NADH oxidation as a change in absorbance at 340 nm.
195 Protein content was determined using a BCA assay kit as described previously
196 ([Hasunuma et al., 2013](#)).

197

198 **2.7 qPCR analysis**

199 *Synechocystis* 6803 cells, cultivated at 30°C and 37°C under anaerobic conditions
200 for 24 h, were harvested by centrifugation at 10,000 × g for 1 min and immediately
201 frozen in liquid nitrogen. Total RNA was extracted from the frozen cells using Fruit-
202 mate for RNA Purification (Takara Bio Inc., Shiga, Japan) and a NucleoSpin RNA kit
203 (Takara Bio Inc.) according to the manufacturer instructions. Complementary DNA
204 was synthesized from 30 ng of total RNA by using a ReverTra Ace qPCR RT Master
205 Mix with gDNA Remover (TOYOBO, Osaka, Japan), and qPCR was performed by
206 using THUNDERBIRD SYBR qPCR Mix (TOYOBO) and Mx qPCR Systems (Agilent
207 Technologies) as previously described ([Ho et al., 2017](#)). The qPCR primers used in
208 this study were as follows: for *rnpB*, 5'-GTGGAACCGCTTGAGGAATTTG-3' and 5'-
209 TTTTGACAGCATGCCACTGG-3', for *ppc*, 5'-ACGATGCCAGTGATGTGTTG-3' and 5'-
210 TTCAAACAGGGGCACAATGC-3', and for *mdh*, 5'-AGATTTGATGCTGCCCTTGC-3' and
211 5'-AGTAAGGCGGCAATTCAGC-3'. Relative transcript levels were evaluated using
212 the level of the *rnpB* encoding RNA subunit of RNase P as a reference, and then

213 normalized by the levels of each gene at 30°C.

214

215

216 3. Results

217 3.1. Increased temperature enhances secretory production of organic acids

218 in *Synechocystis* cells

219 *Synechocystis* 6803 cells were cultivated under photoautotrophic conditions and

220 transferred to dark and anoxic conditions with an initial cell concentration of 5 g-

221 DCW/L to initiate secretion of organic acids by autofermentation. The

222 autofermentation of *Synechocystis* has been so far performed at only 30°C

223 (Hasunuma et al., 2016; Ueda et al., 2016). In Fig. 1, effects of temperature on

224 secretory production of organic acids were investigated after 72 h fermentation.

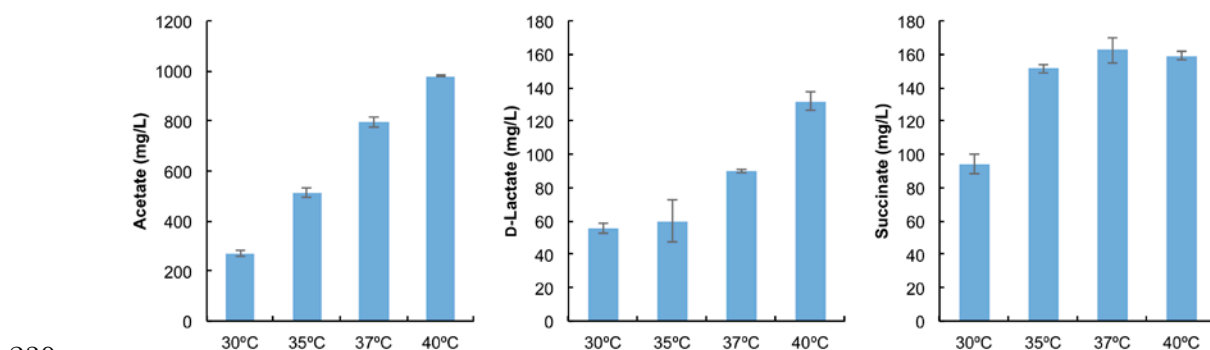
225 Acetate and D-lactate increased with increase in the cultivation temperature. The

226 production of succinate reached a maximum value at 37°C, which was 162.3 mg/L.

227 Other organic acids, which are secreted as minor products, such as fumarate, 2-

228 ketoglutarate, malate, nicotinate, pyruvate and shikimate increased by elevating

229 temperature from 30 to 37°C (Supplementary Table 1).



230

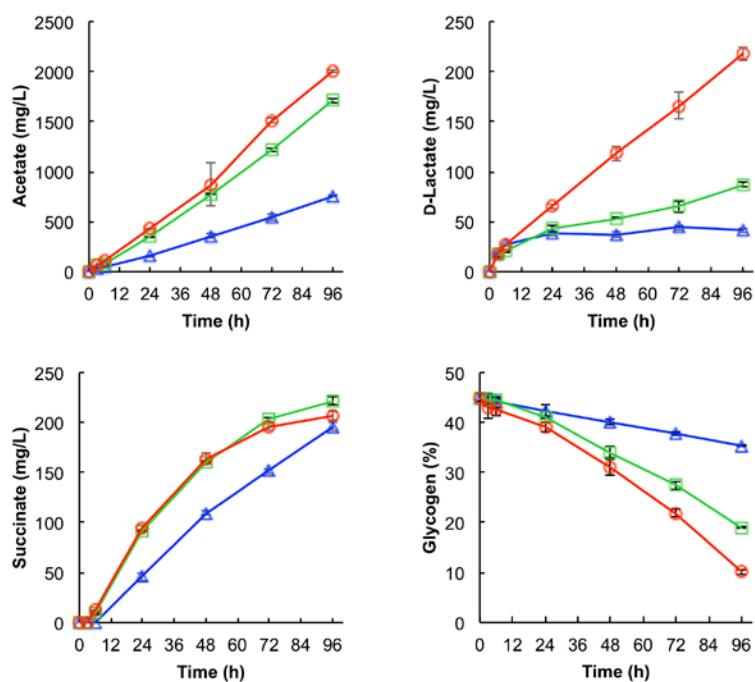
231 **Fig. 1** Organic acid produced after 72 h cultivation at various temperatures. Values

232 represent the average (\pm SD) of three independent experiments.

233

234 In autofermentation, D-lactate and succinate are biosynthesized via sugar
235 catabolism (Hasunuma et al., 2016). The succinate biosynthetic route includes
236 glycolysis, the anaplerotic pathway and the reductive TCA cycle in which PEPC
237 encoded by *ppc* is a rate-limiting enzyme. In fact, overexpression of *ppc* improved
238 succinate production in *Synechocystis* 6803 (Hasunuma et al., 2016). Thus, time-
239 course analysis of organic acid production was carried out using the *ppc*-
240 overexpressing strain, Ppc-ox (Fig. 2). Production of acetate, D-lactate and
241 succinate was enhanced by elevating temperature from 30°C to 37°C. Acetate
242 productivity, shown as the slope of Fig. 2, increased together with the increase in
243 temperature. D-lactate production almost reached a plateau after 9 h cultivation at
244 30°C, while elevated temperature resulted in a continuous increase in D-lactate
245 even after 9 h of cultivation. Secretion of succinate was initiated after 6 h. The
246 initial slopes of succinate production at 35°C and 37°C were higher than that of
247 30°C. Ppc-ox exhibited higher production of acetate, D-lactate and succinate at
248 37°C, relative to that of the wild-type strain.

249



250

251 **Fig. 2** Time-course of organic acid secreted and intracellular glycogen in Ppc-ox
 252 cultivated at 30°C (blue triangles), 35°C (green squares) and 37°C (red circles). Values
 253 represent the average (\pm SD) of three independent experiments.

254

255 The time course of intracellular glycogen content in Ppc-ox was compared
 256 using three different temperatures (Fig. 2). At 30°C, glycogen content decreased
 257 from 43% to 33%. When the cells were cultivated at 35°C and 37°C, glycogen
 258 content decreased to 19% and 11%, respectively after 96 h fermentation. Decrease
 259 in glycogen at higher temperatures was accompanied by reduction in OD₇₅₀ and
 260 less higher density molecules observed with a transmission electron microscope
 261 (TEM), while cell number remained constant (Fig. S1).

262

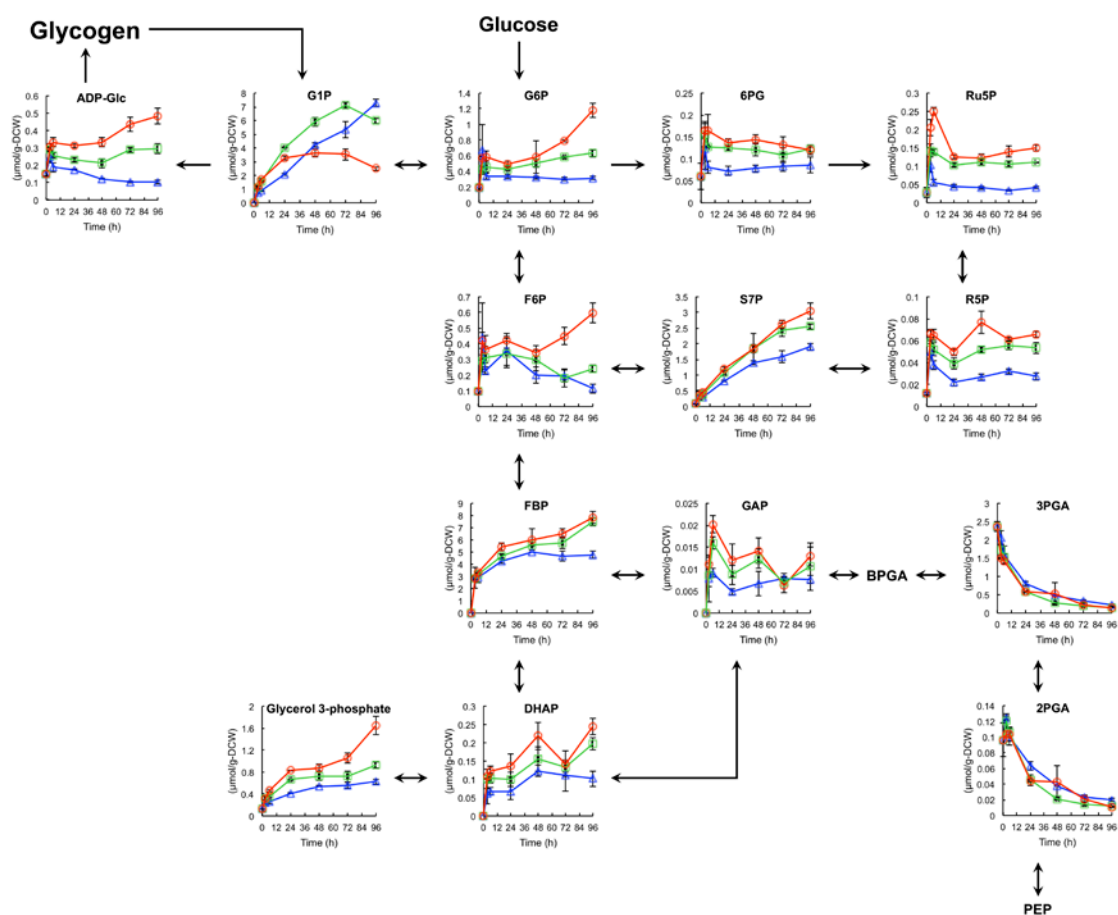
263 3.2. The temporal and temperature dependent metabolome

264 In order to determine the effect of fermentation temperature on dynamic

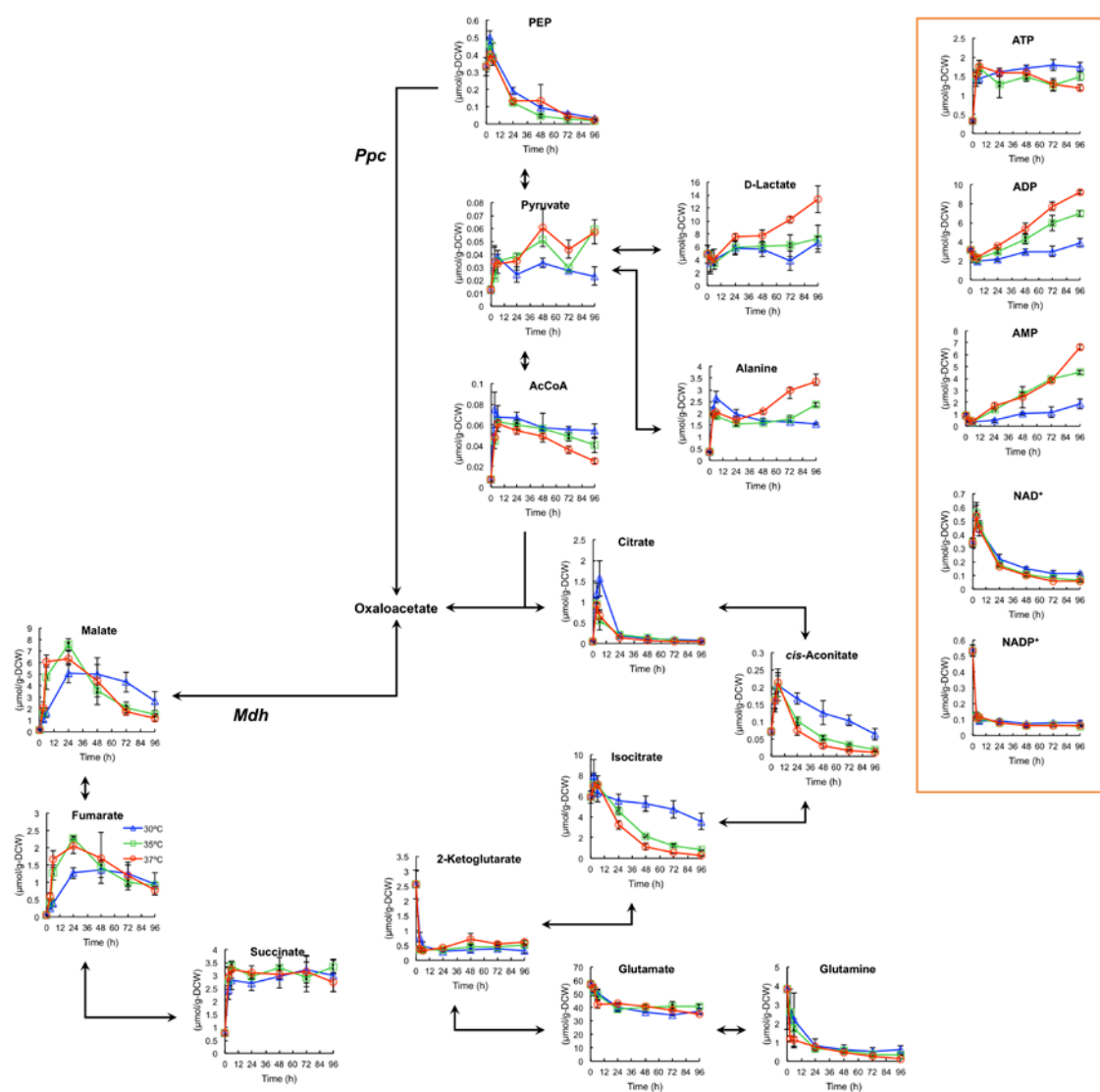
265 metabolism in Ppc-ox, time course analysis of intracellular metabolites was
266 performed during autofermentation at three different temperatures. Metabolites
267 involved in glycolysis, pentose phosphate pathway (PPP), and TCA cycle, as well as
268 metabolism of amino acids, nucleotides and cofactors, are shown in Fig. 3 and Fig.
269 S2. Accumulation of hexose and pentose phosphates such as glucose 6-phosphate
270 (G6P), fructose 6-phosphate (F6P), fructose 1,6-bisphosphate (FBP), 6-
271 phosphogluconate (6PG), ribulose 5-phosphate (Ru5P), ribose 5-phosphate (R5P)
272 and sedoheptulose 7-phosphate (S7P) was dependent of temperature except for
273 glucose 1-phosphate (G1P). G6P, F6P and FBP continued to increase over time at
274 37°C, while they remained almost constant in the latter half of the fermentation at
275 30°C. The pool size of G1P did not increase after 48 h at 37°C. FBP is converted to
276 glyceraldehyde 3-phosphate (GAP) and dihydroxyacetonephosphate (DHAP), which
277 accumulated depending on the temperature. Glycerol 3-phosphate increased along
278 with elevating temperature. The pool size of 3-phosphoglycerate (3PGA), 2-
279 phosphoglycerate (2PGA), and phosphoenolpyruvate (PEP) decreased over time,
280 and this pattern was almost same among the 30°C, 35°C and 37°C groups. Pyruvate,
281 D-lactate and pyruvate-derived amino acids such as alanine, leucine, isoleucine and
282 valine increased dependent on temperature. On the other hand, acetyl-CoA
283 (AcCoA) and metabolites synthesized via the oxidative TCA cycle (including citrate,
284 *cis*-aconitate and isocitrate) decreased with time, and demonstrated lower pool
285 size at higher temperature. Malate, fumarate and succinate synthesized via the
286 reductive TCA cycle demonstrated higher pool size at elevated temperatures until
287 24 h. Arginine, histidine and phenylalanine showed temperature dependent

288 increases in pool size, while proline decreased with increasing temperature.

289 The time course of adenosine phosphate and cofactor pool sizes is shown in
290 Fig. 3. Adenylate energy charge, defined as $[(ATP) + 1/2 (ADP)] / [(ATP) + (ADP) +$
291 $(AMP)]$ (Chapman et al., 1971), decreased along with elevating temperature.
292 Elevated temperature resulted in a slightly lower NAD^+ level than that of 30°C .
293 Reduced $NADH$ and $NADPH$ were not detected with CE-MS due to their low
294 abundance.
295



296



297

298 **Fig. 3** Time course of intracellular metabolite pool size in Ppc-ox cultivated at 30°C
 299 (blue triangles), 35°C (green squares) and 37°C (red circles). Abbreviations: AcCoA,
 300 acetyl-CoA; ADP-Glc, ADP-glucose; BPGA, 1,3-bisphosphoglycerate; DHAP,
 301 dihydroxyacetonephosphate; FBP, fructose 1,6-bisphosphate; F6P, fructose 6-
 302 phosphate; GAP, glyceraldehyde 3-phosphate; G1P, glucose 1-phosphate; G6P,
 303 glucose 6-phosphate; PEP, phosphoenolpyruvate; 6PG, 6-phosphogluconate; 2PGA,
 304 2-phosphoglycerate; 3PGA, 3-phosphoglycerate; R5P, ribose 5-phosphate; Ru5P,
 305 ribulose 5-phosphate; S7P, sedoheptulose 7-phosphate. Values represent the average
 306 (\pm SD) of three independent experiments.

307

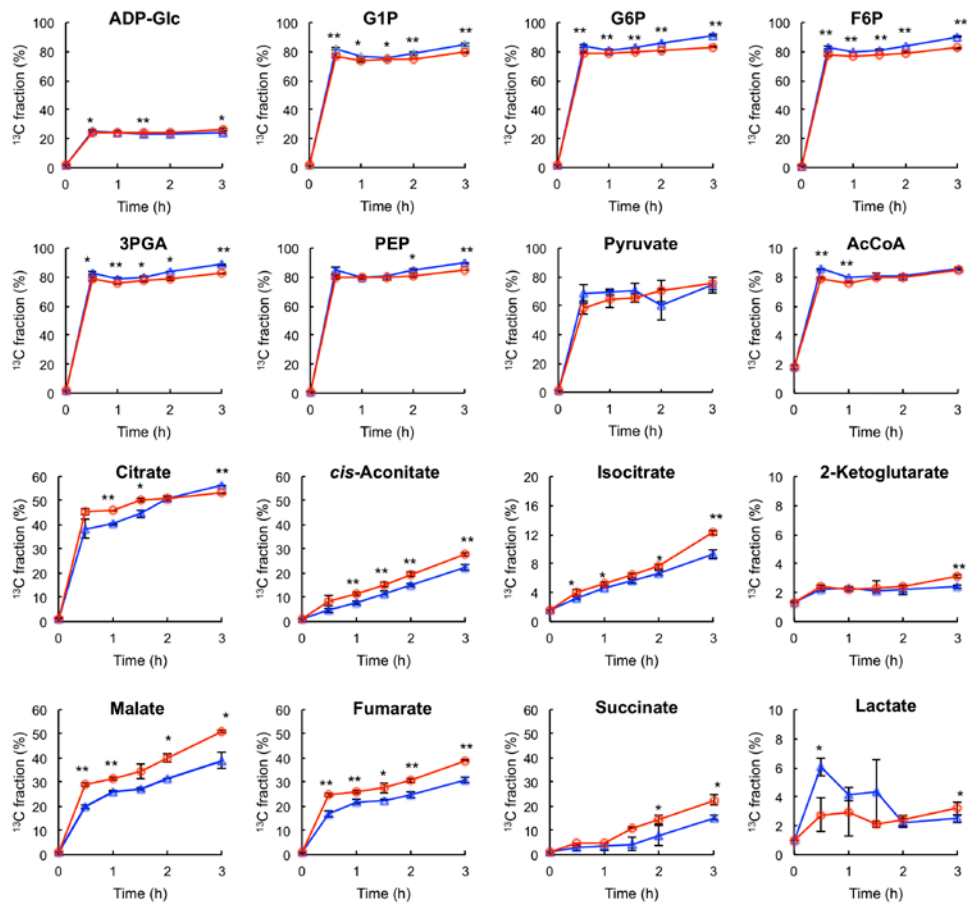
308 **3.3. Metabolite turnover under anaerobic conditions reveals a glycolysis to**
309 **TCA bottleneck**

310 Time course analysis of metabolite pool sizes is insufficient to account for carbon
311 flow and distribution, because the pool size is dependent on the rate of synthesis
312 and utilization of metabolite. Even though a particular reaction is activated under a
313 certain condition, the amount of active metabolite may remain unchanged under
314 steady state conditions.

315 In the present study, to more comprehensively elucidate the effects of
316 elevating temperature on central metabolism, *in vivo* kinetics of carbon
317 assimilation were investigated using [U-¹³C] glucose as a tracer compound. Glucose
318 incorporated into the cells is phosphorylated to G6P by glucokinase (Lee et al.,
319 2005), and then metabolized via glycolysis and PPP.

320 As shown in Fig. 4, metabolites involved in glycolysis and PPP were
321 immediately labeled with ¹³C after the initiation of the autofermentation. The ¹³C
322 fraction is defined as the ratio of ¹³C to total carbon in metabolites, which is
323 obtained by mass spectrometry. Since ADP-glucose, a precursor of glycogen (Fig.
324 3), and G1P are labeled with ¹³C, glucose might be utilized to synthesize glycogen.
325 The incorporation of ¹³C into glycogen was not observed during 3-h ¹³C labeling,
326 which should be due to the large pool size of glycogen.

327



328

329 **Fig. 4** Time-course changes in ^{13}C fractions of metabolites following ^{13}C -glucose
 330 addition to cultures of Ppc-ox cultivated at 30°C (blue triangles) and 37°C (red circles).
 331 Values represent the average (\pm SD) of three independent experiments. Statistical
 332 significance was determined using the Student's *t*-test (* $P < 0.05$, ** $P < 0.01$).

333

334 In cyanobacteria, glycogen is hydrolyzed to G1P by glycogen phosphorylase
 335 (Aikawa et al., 2015), and then converted to G6P by phosphoglucosmutase (Lindahl
 336 and Florencio, 2003). Therefore, both G6P derived from glycogen and ^{13}C -G6P
 337 derived from $[\text{U-}^{13}\text{C}]$ can be utilized as carbon sources for organic acids
 338 biosynthesis.

339 Sugar phosphates including G1P, G6P, and F6P and triose phosphates such

340 as 3PGA demonstrated slightly higher ^{13}C fractions at 30°C relative to that of 37°C,
341 over the course of 3 h fermentation. On the other hand, elevated temperature
342 resulted in significantly higher ^{13}C -fractions of malate, fumarate and succinate
343 when compared to that of 30°C. ^{13}C fractions of pyruvate, lactate, AcCoA, isocitrate
344 and 2-ketoglutarate were similar for both 30°C and 37 °C groups. Increased flux of
345 PEP through the anaplerotic pathway could be clearly observed in the ^{13}C fractions
346 (Fig. S3).

347 ^{13}C enrichment is dependent on the pool size of metabolites. For instance,
348 metabolites whose pool size is large require large amount of ^{13}C to reach high ^{13}C
349 fraction value. Thus, the number of ^{13}C atoms incorporated into metabolites was
350 calculated after 3 h cultivation by multiplying the ^{13}C fraction and pool size (Table
351 1). Oxaloacetate could not be detected due to its low abundance. With exception to
352 G1P, metabolites involved in glycolysis decreased at 37°C relative to that of 30°C. In
353 contrast, ^{13}C atom numbers of malate, fumarate and succinate increased when
354 elevating temperature from 30°C to 37°C. These results indicate enhanced carbon
355 influx to the reductive TCA cycle. Therefore, the metabolic bottleneck that was
356 previously identified (Hasunuma et al., 2016) had become relaxed. This was
357 accompanied by increases in the specific activity of PEPC and MDH (Fig. 5). mRNA
358 levels of *ppc* and *mdh* increased together with the activity of these enzymes which
359 are involved in the carbon influx (Fig. 6). ^{13}C atom number of D-lactate also
360 increased with elevating temperature.

361

362

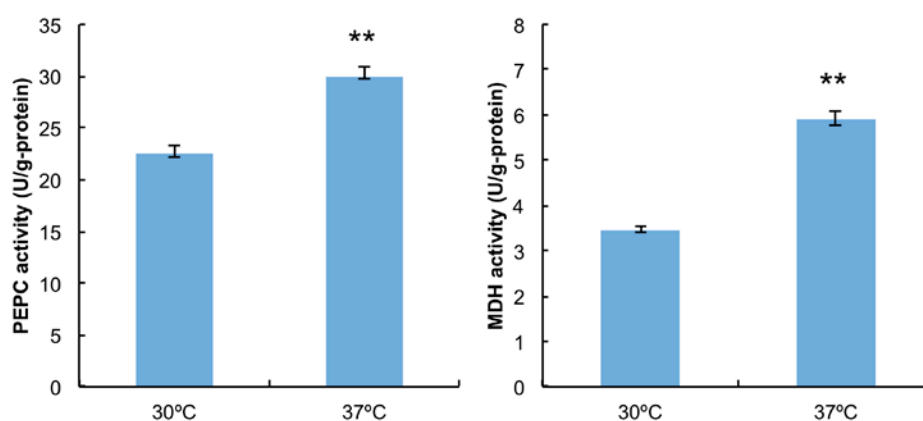
363

364 **Table 1** Number of ¹³C atoms in metabolites.

Metabolite	¹³ C atom number (μmol/g-DCW)	
	30°C	37°C
G1P	501.2 ± 15.8	685.2 ± 45.7*
G6P	274.4 ± 27.5	236.6 ± 16.9
F6P	230.8 ± 7.5	194.6 ± 14.9*
3PGA	667.3 ± 63.6	484.0 ± 35.8*
2PGA	47.2 ± 3.1	38.3 ± 4.2*
PEP	200.3 ± 11.7	149.2 ± 9.4**
Pyruvate	7.1 ± 2.6	5.4 ± 1.3
AcCoA	128.6 ± 18.1	84.7 ± 9.5*
Citrate	444.5 ± 61.4	409.8 ± 10.8
<i>cis</i> -Aconitate	14.7 ± 3.5	10.0 ± 0.5
Isocitrate	392.5 ± 58.3	480.6 ± 86.2
2-Ketoglutarate	7.1 ± 1.2	10.0 ± 0.5*
Malate	170.9 ± 33.5	596.7 ± 121.1*
Fumarate	33.2 ± 6.6	115.2 ± 24.4*
Succinate	157.7 ± 26.9	354.9 ± 60.0*
Lactate	31.0 ± 7.2	59.2 ± 11.7*

365 The number of ¹³C atoms incorporated into metabolites was measured 3 h after addition of ¹³C-
 366 glucose by multiplying the ¹³C fraction, pool size and carbon number. Values represent the
 367 average (± SD) of three independent experiments. Statistical significance was determined using
 368 the Student's *t*-test (**P* < 0.05, ***P* < 0.01).

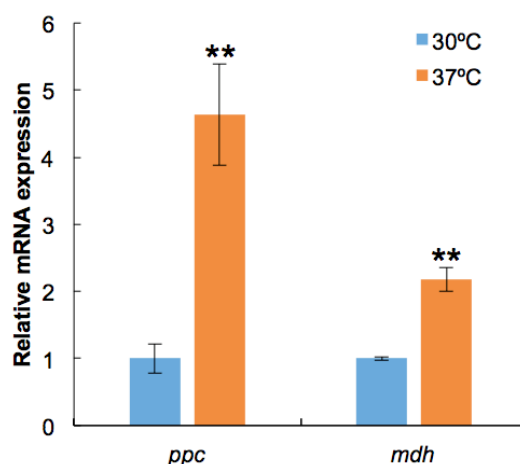
369



370

371 **Fig. 5** Phosphoenolpyruvate carboxylase (PEPC) and malate dehydrogenase (MDH)
 372 specific activities measured after 24 h fermentation. Values represent the average (±
 373 SD) of three independent experiments. Statistical significance was determined using
 374 the Student's *t*-test (***P* < 0.01).

375



376

377 **Fig. 6** Relative expression levels of *ppc* and *mdh* at 30°C and 37°C. Relative transcript
378 levels were evaluated using the level of *mpB* as a reference, and then normalized by
379 the levels of each gene at 30°C. Values represent the average (\pm SD) of three
380 independent experiments. Statistical significance was determined using the Student's *t*-
381 test (** $P < 0.01$).

382

383

384 In Fig. 4, the initial slope of ^{13}C -fraction indicates turnover of metabolites.
385 Organic acids showed slower turnover than sugar phosphates and triose
386 phosphates at both temperatures. Therefore, a bottleneck is still present at one of
387 the reactions between glycolysis and the TCA cycle in Ppc-ox grown at 37°C.

388

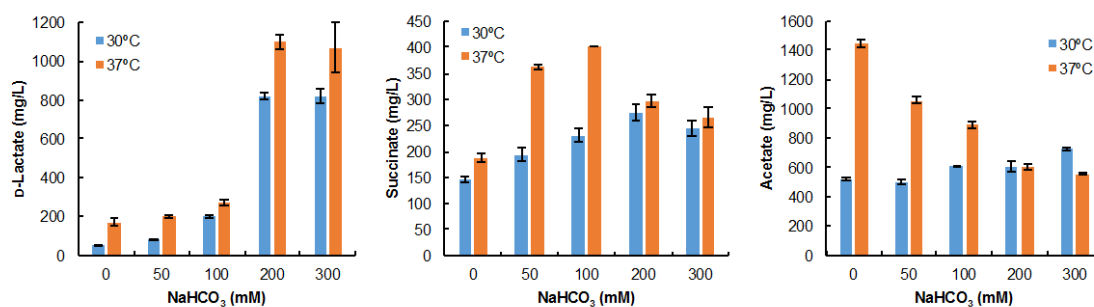
389

390 **3.4. Improvement of succinate bioproduction**

391 PEPC forms the TCA intermediate oxaloacetate via reaction of the glycolysis
392 intermediate PEP with bicarbonate. In order to improve succinate production from

393 the TCA cycle, sodium bicarbonate was added to the fermentation. As shown in Fig.
 394 7, an additive effect of high temperature and NaHCO₃ addition on the secretory
 395 production of D-lactate and succinate was observed. Succinate production was the
 396 highest (400.8 mg/L) in the presence of 100 mM NaHCO₃ at 37°C in Ppc-ox. The
 397 highest D-lactate (1,097.9 mg/L) titer was obtained in the presence of 200 mM
 398 NaHCO₃. The addition of up to 300 mM NaHCO₃ resulted in increases of pH from 7.6
 399 to no higher than 7.8.

400



401

402 **Fig. 7** Effect of NaHCO₃ addition on D-lactate, succinate and acetate production after
 403 72 hours fermentation. Bars on the left hand side in blue and bars on the right hand
 404 side in orange indicate concentrations at 30°C and 37°C, respectively. Values represent
 405 the average (\pm SD) of three independent experiments.

406

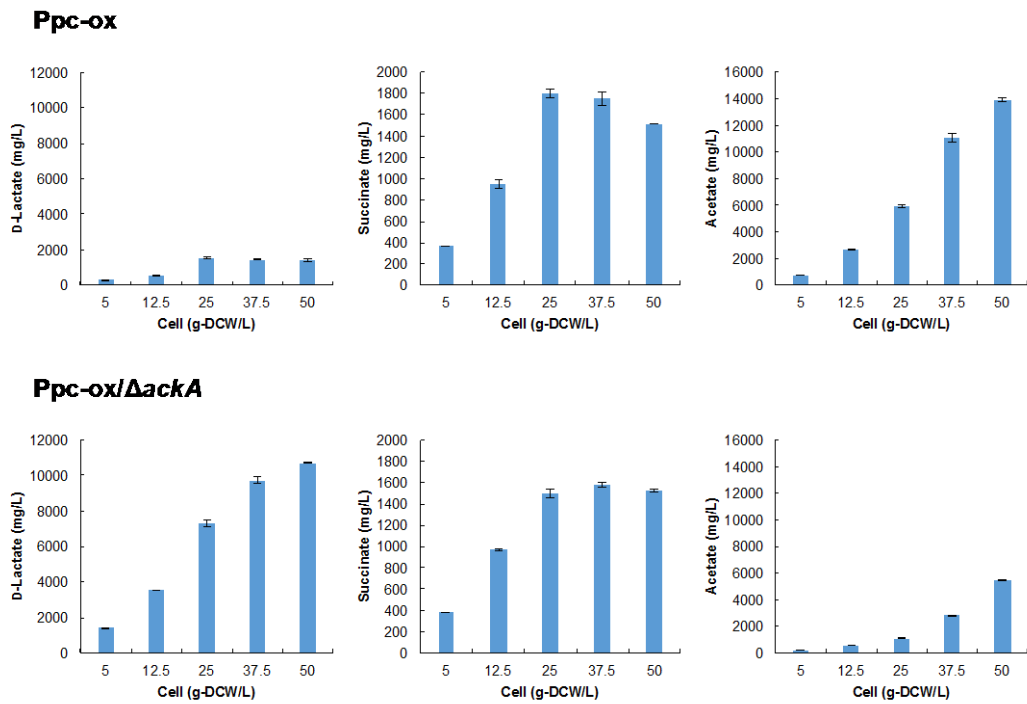
407 Effect of initial cell concentration on D-lactate and succinate production
 408 was also investigated at 37°C in the presence of 100 mM NaHCO₃ (Fig. 8).
 409 Production of D-lactate and succinate was dependent on the initial cell
 410 concentration, with the highest concentration of D-lactate (1,520.3 mg/L) and
 411 succinate (1,802.3 mg/L) produced using 25 g-DCW/L (Fig. 8). Both succinate and
 412 lactate titers stopped improving after the initial cell concentration was increased to

413 over 25 g-DCW/L.

414 Since acetate was a major byproduct during succinate production, further
415 optimization of succinate and lactate production was investigated by knocking out
416 the acetate kinase (AK) gene (*ackA*, sll1299) in the Ppc-ox strain. This resulted in
417 significantly lower production of acetate byproduct, while D-lactate production
418 increased to 10.7 g/L, the highest reported titer in cyanobacteria (Fig. 8, lower
419 panels). Although succinate production in Ppc-ox/ Δ *ackA* decreased when using cell
420 densities of 25 and 37.5 g-DCW/L, succinate levels slightly increased when using 5,
421 12.5 and 50 g-DCW/L. Interestingly, without *ackA*, levels of PEP, pyruvate and
422 AcCoA all increased which is consistent with higher lactate production (Fig. 9).
423 Despite the increases in lactate and succinate production, knockout of *ackA* did not
424 affect culture pH. This may be due to the presence of 100 mM Hepes-KOH, pH 7.8,
425 or by the additional NaHCO₃ during increased lactate production.

426

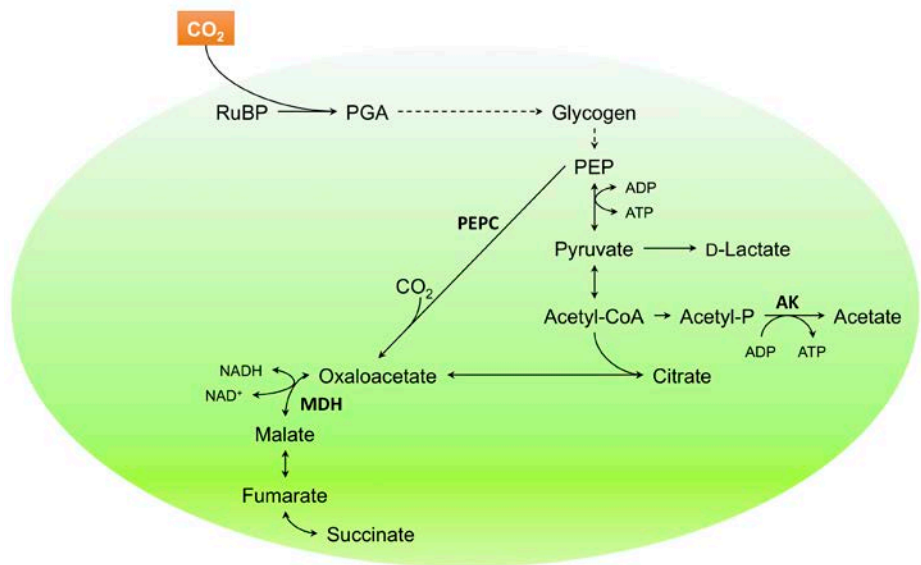
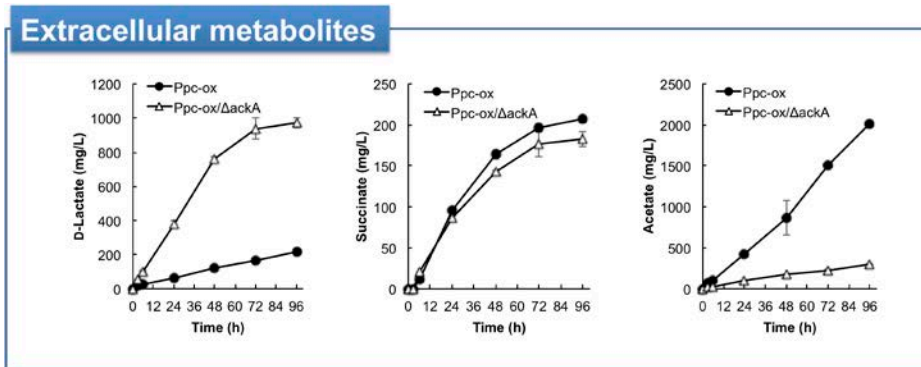
427



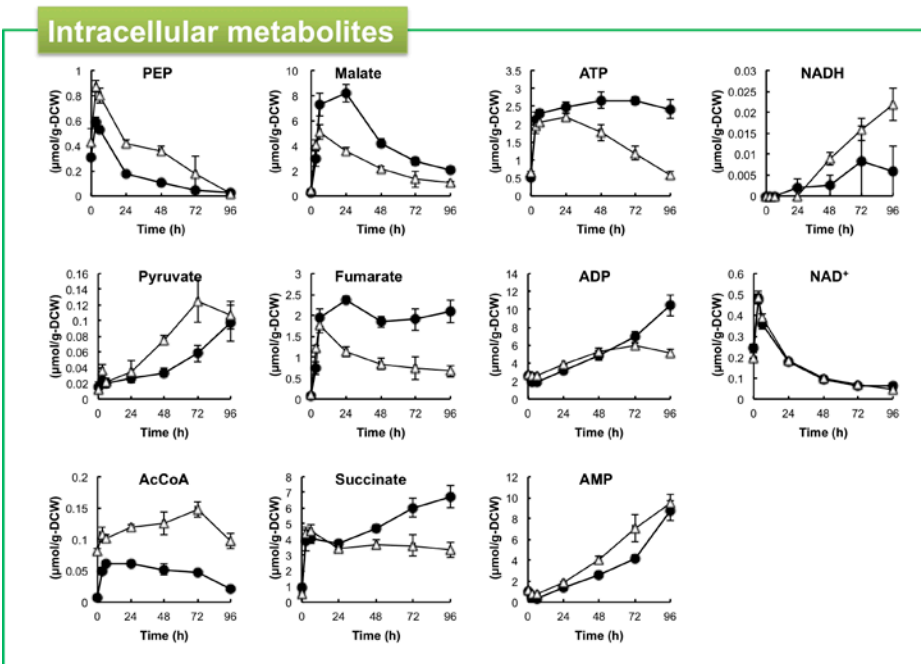
428

429 **Fig. 8** D-lactate, succinate and acetate produced after 72 hours fermentation at 37°C
 430 using 100 mM NaHCO₃ and various initial cell concentrations. Organic acid production
 431 in the Ppc-ox strain is shown in the upper 3 panels, and production in the *ackA*
 432 knockout of Ppc-ox is shown in the lower 3 panels. Values represent the average (±
 433 SD) of three independent experiments.

434



435



436

437

438

Fig. 9 Time-course of organic acid secretion and intracellular metabolites in Ppc-ox (closed circles, also shown in Fig. 2) and Ppc-ox/ΔackA (open triangles) cultivated

439 anaerobically at 37°C without NaHCO₃ supplementation. Values represent the average
440 (\pm SD) of three independent experiments. Effects of *ackA* deletion on organic acid
441 production are shown in the upper panel, and effects on related intracellular
442 metabolites are shown in the lower two panels. The middle panel shows the pathway to
443 succinate discussed in this study.

444

445

446 **4. Discussion**

447 In this study, temperature enhanced secretory production of organic acids
448 in *Synechocystis* 6803 was observed under dark anoxic conditions. A metabolomics
449 approach unveiled dynamic variations in the pool size and turnover of metabolites
450 dependent on the fermentation temperature. To the best of our knowledge, this is
451 the first comprehensive temperature dependent metabolomics study of a
452 microorganism (Yurkovich et al., 2017).

453 Analysis of ¹³C-fraction turnover indicates that a bottleneck between PEP
454 and the TCA cycle was relaxed by increasing temperature from 30°C to 37°C (Fig.
455 4). The pool size of citrate, *cis*-aconitate and isocitrate was lower at 37°C, while
456 malate, fumarate and succinate were increased by elevating temperature during 24
457 h fermentation (Fig. 3). ¹³C atom number of malate, fumarate and succinate greatly
458 increased with elevating temperature (Table 1). The TCA cycle in *Synechocystis*
459 6803 is branched into oxidative and reductive routes. These results suggest that
460 increase in temperature boosts the reductive TCA cycle to produce succinate.

461 A few studies have reported effects of temperature on bioproduction. For
462 example, production of succinate in *E. coli* strain SBS550MG was not significantly

463 affected by temperatures of 37°C or 43°C, whereas glucose concentration, CO₂
464 concentration, pH and cell density were all found to be important factors (Martínez
465 et al., 2011). For production of ascorbic acid-2-phosphate in *Brevundimonas*
466 *diminuta*, cell density, pH and temperature were key variables, with an optimal
467 temperature of 40°C (Shin et al., 2007). Increase in temperature from 33 to 39.5°C
468 was found to induce glutamate production in *Corynebacterium glutamicum*
469 (Gourdon and Lindley, 1999). However, the metabolic pathways underlying the
470 effects of temperature increase on bioproduction have not been comprehensively
471 investigated.

472 In the current study, glycogen was produced during photosynthesis,
473 followed by utilization of glycogen and carbon dioxide as carbon sources.
474 Overexpression of *ppc* increased glycogen utilization to 89% and also improved
475 succinate production at 37°C. Throughout fermentation cell density remained
476 constant while OD₇₅₀ and TEM observed high density particles both decreased,
477 indicating the consumption of glycogen (Fig. S1). Although the optimal
478 temperature of *Synechocystis* 6803 PEPC was reported to be 30°C, the enzyme
479 retained 80% of its activity at 40°C and was tolerant to allosteric inhibition (Takeya
480 et al., 2017).

481 Global transcriptional analysis of *E. coli* indicates that a decrease in
482 temperature from 37°C to 28°C results in an increase in TCA cycle encoding
483 enzymes (Gadgil et al., 2005). Conversely, a 30°C to 45°C temperature increase led
484 to increased glycolytic flux, decreased flux from the TCA cycle into anabolic
485 pathways, and a decrease in adenylate energy charge (Wittmann et al., 2007).

486 AMP and ADP allosterically activate the *E. coli* glycolytic enzymes pyruvate
487 kinase II (Kotlarz et al., 1975) and phosphofructokinase I (Babul, 1978),
488 respectively (Li et al., 2017). Additionally, oxidative phosphorylation generates ATP
489 from NADH, which inhibits *E. coli* citric acid enzymes pyruvate dehydrogenase
490 (Kim et al., 2008) and citrate synthase (Talgoy and Duckworth, 1979; Weitzman,
491 1981). Thus, higher concentrations of ATP slow down central metabolism (Kihira
492 et al., 2011), and a 10% decrease in ATP concentration was enough to exert a
493 beneficial effect on succinate production (Li et al., 2017). Reduction of anaerobic
494 ATP levels via PEP synthase mediated futile cycling was also critical to obtain the
495 impressive heterotrophic succinate titer of 31.87 g/L (Li et al., 2017). Accordingly,
496 in the current study, increasing temperature to 37°C had a dramatic effect on the
497 increase of ADP and AMP concentrations, and a moderate but significant effect on
498 lowering ATP level. Therefore, the current study further emphasizes that lowering
499 adenylate energy charge is an effective strategy for increasing autotrophic
500 succinate yields.

501 Reducing anaerobic NADH/NAD⁺ ratio by overexpression of the fumarate
502 reductase gene was reported to be important for increasing succinate yield in *E.*
503 *coli* (Li et al., 2017). A high NADH/NAD⁺ ratio has also been reported to have a
504 negative effect on bioproducton of glutamate in *C. glutamicum* (Gourdon and
505 Lindley, 1999). Conversely, in the cyanobacteria *Synechococcus* sp. PCC 7002,
506 knockout of nitrate reductase led to an increase in NADH/NAD⁺ ratio as well as
507 glycogen, H₂, lactate and glycogen production (Qian et al., 2016). Cyanobacteria
508 nitrogen reduction normally leads to NADH consumption and catabolism of

509 glycogen via glycogen phosphorylase and phosphoglucomutase. Accordingly,
510 glycogen metabolism and NADH/NAD⁺ ratio should be carefully investigated and to
511 further optimize the autotrophic production of succinate.

512 Under anaerobic conditions cyanobacteria run their TCA cycle backwards
513 from oxaloacetate to succinate (Fig. 9), which generates NAD⁺ from NADH. In this
514 study, overexpression of *ppc* in the metabolically engineered strain Ppc-ox provides
515 more oxaloacetate for this route. Additional *ackA* knockout in Ppc-ox results in
516 increased levels of glycolytic intermediates PEP, pyruvate and AcCoA, while TCA
517 intermediates to succinate decreased (Fig. 9). This indicates that in the Ppc-ox *ackA*
518 knockout PEPC can no longer overcome the glycolysis to TCA bottleneck mentioned
519 above, and therefore additional overexpression of the pyruvate carboxylase (PC)
520 gene may be useful to further increase succinate titers (Meng et al., 2016). As
521 NADH levels also increase in the Ppc-ox *ackA* knockout, the overexpression of
522 malate dehydrogenase or NADH dependent fumarate reductase genes are
523 additional options to improve succinate production while at the same time
524 decreasing NADH/NAD⁺ ratio (Li et al., 2017).

525 Previous knockout of *ackA* together with overexpression of *SigE* and 200
526 mM KCl supplementation in *Synechococcus* 6803 resulted in an increase of
527 succinate titers up to 141 mg/L and an increase of lactate titers up to 217.6 mg/L
528 (Table 2, Ueda et al., 2016). In the current report, knockout of *ackA* further
529 improved succinate titers over 10 fold using *Synechocystis* 6803 Ppc-ox. Although
530 impressive succinate titers have been achieved using heterotrophic *E. coli* grown
531 with glucose as an energy source (Li et al., 2017), production in autotrophic cells

532 must be optimized in order to develop a renewable process. Cyanobacteria
 533 succinate production has previously been optimized using a variety of strategies
 534 (Table 2). Using only photosynthetic conditions, succinate levels could be increased
 535 further in *Synechococcus elongatus* PCC 7942 to 430 mg/L (Lan et al., 2016). In the
 536 current autotrophic study, the highest autotrophic succinate titer of 1.8 g/L was
 537 achieved using the metabolically engineered strain Ppc-ox with overexpression of
 538 *ppc* in combination with a straightforward approach of carbon dioxide utilization,
 539 and elevation of fermentation temperatures to 37°C.

540

541

542

543 **Table 2** Comparison of cyanobacteria succinate bioproduction studies.

Study	Organism	Conditions	Succinate Titer (Cultivation time)	Succinate Productivity (Cultivation time used for calculation)
Li et al., 2016	<i>Synechococcus elongatus</i> PCC 7942	Photosynthetic, nitrogen starvation, Δglc , + <i>glcA</i> , + <i>ppc</i>	435.0 µg/L (48 h)	9 µg/L/h (0-48 h)
Huang et al., 2016	<i>Synechococcus elongatus</i> PCC 7942	Photosynthetic, nitrogen starvation, repression of <i>glc</i> , <i>sdhA</i> , <i>sdhB</i>	580-630 µg/L (48 h)	13 µg/L/h (0-48 h)
Osanai et al., 2015	<i>Synechococcus</i> sp. PCC 6803	Dark anaerobic, + <i>sigE</i> , $\Delta ackA$	~115 mg/L (96 h)	1.38 mg/L/h (0-96 h)
Ueda et al., 2016	<i>Synechococcus</i> sp. PCC 6803	Dark anaerobic, + <i>sigE</i> , $\Delta ackA$, 200 mM KCl	141.0 mg/L (72 h)	2 mg/L/h (0-72 h)
Lan et al., 2016	<i>Synechococcus elongatus</i> PCC 7942	Photosynthetic, overexpression of 4 genes*	430 mg/L (192 h)	3.33 mg/L/h (72-96 h)
This study	<i>Synechocystis</i> sp. PCC 6803	Dark anoxic, Ppc-ox, NaHCO ₃ , 37°C	1.8 g/L (72 h)	25 mg/L/h (0-72 h)

544 *The study by Lan et al. utilized overexpression of α-ketoglutarate decarboxylase,

545 succinate semialdehyde dehydrogenase, citrate synthase and PEPC genes.

546

547

548 **Acknowledgements**

549 The authors thank Ms. Ryoko Yamazaki and Ms. Yui Tamagaki for their technical
550 assistance. This work was supported by Advanced Low Carbon Technology
551 Research and Development Program (ALCA) from the Japan Science and
552 Technology Agency (JST), the Ministry of Education, Culture, Sports, Science, and
553 Technology (MEXT), Japan. This work was also supported by JSPS KAKENHI Grant
554 Number JP15H05557.

555

556

557 **References**

558 Aikawa, S., Ho, S.H., Nakanishi, A., Chang, J.S., Hasunuma, T., Kondo, A. 2015.
559 Improving polyglucan production in cyanobacteria and microalgae via cultivation
560 design and metabolic engineering. *Biotechnol. J.* 10, 886-898.

561

562 Aikawa, S., Joseph, A., Yamada, R., Izumi, Y., Yamagishi, T., Matsuda, F., Kawai, H.,
563 Chang, J.S., Hasunuma, T., Kondo, A. 2013. Direct conversion of *Spirulina* to ethanol
564 without pretreatment or enzymatic hydrolysis processes. *Energy Environ. Sci.* 6,
565 1844-1849.

566

567 Akhtar, J., Idris, A., Abd. Aziz, R., 2014. Recent advances in production of succinic
568 acid from lignocellulosic biomass. *Appl. Microbiol. Biotechnol.* 98, 987-1000.

569

570 Angermayr, S.A., Gorchs Rovira, A., Hellingwerf, K.J., 2015. Metabolic engineering of
571 cyanobacteria for the synthesis of commodity products. *Trends Biotechnol.* 33,
572 352-361.

573

574 Babul, J., 1978. Phosphofructokinases from *Escherichia coli*. *J. Biol. Chem.* 253,
575 4350-4355.

576

577 Chapman, A.G., Fall, L., Atkinson, D.E., 1971. Adenylate energy charge in *Escherichia*
578 *coli* during growth and starvation. *J. Bacteriol.* 108, 1072-1086.

579

580 Choi, S., Song, C.W., Shin, J.H., Lee, S.Y., 2015. Biorefineries for the production of top
581 building block chemicals and their derivatives. *Metab. Eng.* 28, 223-239.
582

583 Delhomme, C., Weuster-Botz, D., Kühn, F.E., 2009. Succinic acid from renewable
584 resources as a C4 building-block chemical – a review of the catalytic possibilities in
585 aqueous media. *Green Chem.* 11, 13-26.
586

587 Dismukes, G.C., Carrieri, D., Bennette, N., Ananyev, G.M., Posewitz, M.C., 2008.
588 Aquatic phototrophs: efficient alternatives to land-based crops for biofuels. *Curr.*
589 *Opin. Biotechnol.* 19, 235–240.
590

591 Formighieri, C., Melis, A., 2015. A phycocyanin center dot phellandrene synthase
592 fusion enhances recombinant protein expression and β -phellandrene
593 (monoterpene) hydrocarbons production in *Synechocystis* (cyanobacteria). *Metab.*
594 *Eng.* 32, 116–124.
595

596 Gadgil, M., Kapur, V., Hu, W.S., 2005. Transcriptional response of *Escherichia coli* to
597 temperature shift. *Biotechnol. Prog.* 5, 41-44.
598

599 Gourdon, P., Lindley, N.D., 1999. Metabolic analysis of glutamate production by
600 *Corynebacterium glutamicum*. *Metab. Eng.* 1, 224-231.
601

602 Hasunuma, T., Matsuda, M., Kondo, A., 2016. Improved sugar-free succinate
603 production by *Synechocystis* sp. PCC 6803 following identification of the limiting
604 steps in glycogen catabolism. *Metab. Eng. Commun.* 3, 130-141.
605

606 Hasunuma, T., Matsuda, M., Senga, Y., Aikawa, S., Toyoshima, M., Shimakawa, G.,
607 Miyake, C., Kondo, A., 2014. Overexpression of *flv3* improves photosynthesis in the
608 cyanobacterium *Synechocystis* sp. PCC 6803 by enhancement of alternative
609 electron flow. *Biotechnol. Biofuel.* 7, 493.
610

611 Ho, S.H., Nakanishi, A., Kato, Y., Yamasaki, H., Chang, J.S., Misawa, N., Hirose, Y.,
612 Minagawa, J., Hasunuma, T., Kondo, A., 2017. Dynamic metabolic profiling together
613 with transcription analysis reveals salinity-induced starch-to-lipid biosynthesis in
614 alga *Chlamydomonas* sp. *JSC4, Sci. Rep.* 7: 45471.
615

616 Huang, C.H., Shen, C.R., Li, H., Sung, L.Y., Wu, M.Y., Hu, Y.C., 2016. CRISPR
617 interference (CRISPRi) for gene regulation and succinate production in
618 cyanobacterium *S. elongatus* PCC 7942. *Microb. Cell Fact.* 15, 196.
619

620 Iijima, H., Nakaya, Y., Kuwahara, A., Hirai, M.Y., Osanai, T., 2015. Seawater
621 cultivation of freshwater cyanobacterium *Synechocystis* sp. PCC 6803 drastically
622 alters amino acid composition and glycogen metabolism. *Front. Microbiol.* 6, 326.
623

624 Ikada, Y., Jamshidi, K., Tsuji, H., Hyon, S.H., 1987. Stereocomplex formation between
625 enantiomeric poly (lactides). *Macromolecules* 20, 904–906.

626
627 Kaneko, T., Sato, S., Kotani, H., Tanaka, A., Asamizu, E., Nakamura, Y., Miyajima, N.,
628 Hirosawa, M., Sugiura, M., Sasamoto, S., Kimura, T., Hosouchi, T., Matsuno, A.,
629 Muraki, A., Nakazaki, N., Naruo, K., Okumura, S., Shimpo, S., Takeuchi, C., Wada, T.,
630 Watanabe, A., Yamada, M., Yasuda, M., Tabata, S., 1996. Sequence analysis of the
631 genome of the unicellular cyanobacterium *Synechocystis* sp. strain PCC 6803. II.
632 Sequence determination of the entire genome and assignment of potential protein-
633 coding region. DNA Res. 3, 109–136.
634
635 Kihira, C., Hayashi, Y., Azuma, N., Noda, S., Maeda, S., Fukiya, S., Wada, M.,
636 Matsushita, K., Yokota, A. 2012. Alterations of glucose metabolism in *Escherichia*
637 *coli* mutants defective in respiratory-chain enzymes. J. Bacteriol. 158, 215-223.
638
639 Kim, Y., Ingram, L.O., Shanmugam, K.T., 2008. Dihydrolipoamide dehydrogenase
640 mutation alters the NADH sensitivity of pyruvate dehydrogenase complex of
641 *Escherichia coli* K-12. J. Bacteriol. 190, 3851–3858.
642
643 Kotlarz, D., Garreau, H., Buc, H., 1975. Regulation of the amount and of the activity
644 of phosphofructokinases and pyruvate kinases in *Escherichia coli*. Biochim.
645 Biophys. Acta. 381, 257–268.
646
647 Lai, M.C., Lan, E.I., 2015. Advances in metabolic engineering of cyanobacteria for
648 photosynthetic biochemical production. Metabolites 5, 636–658.
649
650 Lan, E.I., Wei, C.T., 2016. Metabolic engineering of cyanobacteria for the
651 photosynthetic production of succinate. Metab. Eng. 38, 483-493.
652
653 Lee, J.M., Ryu, J.Y., Kim, H.H., Choi, S.B., de Marsac, N.T., Park, Y.I., 2005.
654 Identification of a glucokinase that generates a major glucose phosphorylation
655 activity in the cyanobacterium *Synechocystis* sp. PCC 6803. Mol. Cells 19, 256-261.
656
657 Li, J., Li, Y., Cui, Z., Liang, Q., Qi, Q., 2017. Enhancement of succinate yield by
658 manipulating NADH/NAD⁺ ratio and ATP generation. Appl. Microbiol. Biotechnol.
659 101, 3153-3161.
660
661 Li, H., Shen, C.R., Huang, C.H., Sung, L.Y., Wu, M.Y., Hu, Y.C., 2016. CRISPR-Cas9 for
662 the genome engineering of cyanobacteria and succinate production. Metab. Eng. 38,
663 293-302.
664
665 Lindahl, M., Florencio, F.J., 2003. Thioredoxin-linked processes in cyanobacteria
666 are as numerous as in chloroplasts, but targets are different. Proc. Natl. Acad. Sci.
667 U.S.A. 100, 16107-16112.
668
669 Martínez, I., Lee, A., Bennett, G.N., San, K.Y., 2011. Culture conditions' impact on
670 succinate production by a high succinate producing *Escherichia coli* strain.
671 Biotechnol. Prog. 27, 1225-1231.

672
673 Meng, J., Wang, B., Liu, D., Chen, T., Wang, Z., Zhao, X., 2016. High-yield anaerobic
674 succinate production by strategically regulating multiple metabolic pathways
675 based on stoichiometric maximum in *Escherichia coli*. *Microb. Cell. Fact.* 15, 141.
676
677 McNeely, K., Xu, Y., Bennette, N., Bryant, D.A., Dismukes, G.C., 2010. Redirecting
678 reductant flux into hydrogen production via metabolic engineering of fermentative
679 carbon metabolism in a Cyanobacterium. *Appl. Environ. Microbiol.* 76, 5032-5038.
680
681 Osanai, T., Shirai, T., Iijima, H., Nakaya, Y., Okamoto, M., Kondo, A., Hirai, M.Y., 2015.
682 Genetic manipulation of a metabolic enzyme and a transcriptional regulator
683 increasing succinate excretion from unicellular cyanobacterium. *Front. Microbiol.*
684 6, 1064.
685
686 Qian, X., Kim, M.K., Kumaraswamy, G.K., Agarwal, A., Lun, D.S., Dismukes, G.C., 2016.
687 Inactivation of nitrate reductase alters metabolic branching of carbohydrate
688 fermentation in the cyanobacterium *Synechococcus* sp. strain PCC 7002. *Biotechnol.*
689 *Bioeng.* 113, 979-988.
690
691 Shin, W.J., Kim, B.Y., Bang, W.G., 2007. Optimization of ascorbic acid-2-phosphate
692 production from ascorbic acid using resting cell of *Brevundimonas diminuta*. *J.*
693 *Microbiol. Biotechnol.* 17, 769-773.
694
695 Takeya, M., Hirai, M.Y., Osanai, T., 2017. Allosteric inhibition of
696 phosphoenolpyruvate carboxylases is determined by a single amino acid residue in
697 cyanobacteria. *Sci. Rep.* 7, 41080.
698
699 Talgoy, M.M., Duckworth, H.W., 1979. The interactions of adenylates with allosteric
700 citrate synthase. *Can. J. Biochem.* 57, 385-395.
701
702 Tasaka, Y., Gombos, Z., Nishiyama, Y., Mohanty, P., Ohba, T., Ohki, K., Murata, N.,
703 1996. Targeted mutagenesis of acyl-lipid desaturases in *Synechocystis*: evidence for
704 the important roles of polyunsaturated membrane lipids in growth, respiration
705 and photosynthesis. *EMBO J.* 15, 6416-6425.
706
707 Rippka, R., Deruelles, J., Waterbury, J.B., Herdman, M., Stanier, R.Y., 1979. Generic
708 assignments, strains histories and properties of pure culture of cyanobacteria. *J.*
709 *Gen. Microbiol.* 111, 1-61.
710
711 Shin, W.J., Kim, B.Y., Bang, W.G., 2007. Optimization of ascorbic acid-2-phosphate
712 production from ascorbic acid using resting cell of *Brevundimonas diminuta*. *J.*
713 *Microbiol. Biotechnol.* 17, 769-773.
714
715 Ueda, S., Kawamura, Y., Iijima, H., Nakajima, M., Shirai, T., Okamoto, M., Kondo, A.,
716 Hirai, M.Y., Osanai, T., 2016. Anionic metabolite biosynthesis enhanced by
717 potassium under dark, anaerobic conditions in cyanobacteria. *Sci. Rep.* 6, 32354.

718
719 Wang, Y., Sun, T., Gao, X., Shi, M., Wu, L., Chen, L., Zhang, W., 2016. Biosynthesis of
720 platform chemical 3-hydroxypropionic acid (3-HP) directly from CO₂ in
721 cyanobacterium *Synechocystis* sp. PCC 6803. *Metab. Eng.* 34, 60–70.
722
723 Wee, Y.J., Kim, J.N., Ryu, H.W., 2006. Biotechnological production of lactic acid and
724 its recent applications. *Food Technol. Biotechnol.* 44, 163–172.
725
726 Weitzman, P.D.J., 1981. Unity and diversity in some bacterial citric acid-cycle
727 enzymes. *Adv. Microb. Physiol.* 22, 185–244.
728
729 Wijffels, R.H., Kruse, O., Hellingwerf, K.J., 2013. Potential of industrial biotechnology
730 with cyanobacteria and eukaryotic microalgae. *Curr. Opin. Biotechnol.* 24, 405–413.
731
732 Williams, J.G.K., 1988. Construction of specific mutations in photosystem II
733 photosynthetic reaction center by genetic engineering methods in *Synechocystis*
734 6803. *Methods Enzymol.* 167, 766–778.
735
736 Wittmann, C., Weber, J., Betiku, E., Krömer, J., Böhm, D., Rinas, U., 2007. Response of
737 fluxome and metabolome to temperature-induced recombinant protein synthesis
738 in *Escherichia coli*. *J. Biotechnol.* 132, 375–384.
739
740 Yurkovich, J.T., Zielinski, D.C., Yang, L., Paglia, G., Rolfsson, O., Sigurjónsson, Ó.E.,
741 Broddrick, J.T., Bordbar, A., Wichuk, K., Brynjólfsson, S., Palsson, S., Gudmundsson,
742 S., Palsson, B.O., 2017. Quantitative time-course metabolomics in human red blood
743 cells reveal the temperature dependence of human metabolic networks. *J. Biol.*
744 *Chem.* 292, 19556–19564.
745

746 **Supplementary Materials**

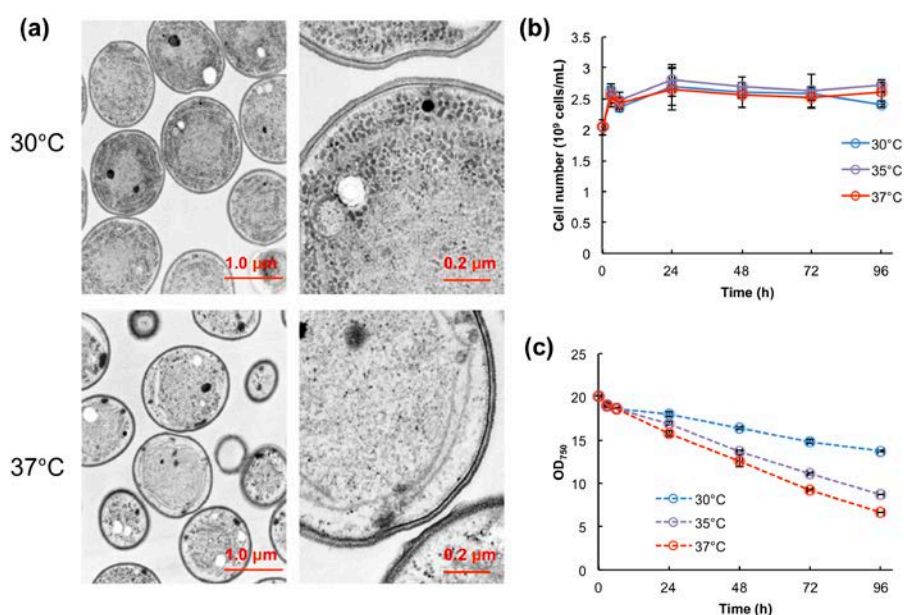
747 **Supplementary Table 1** Organic acid produced after 72 h cultivation at 30°C and
 748 37°C. Values represent the average (\pm SD) of three independent experiments.
 749 Statistical significance was determined using the Student's *t*-test (**P* < 0.05, ***P* <
 750 0.01).

751

Organic acid	Production (mg/L)	
	30°C	37°C
Fumarate	11.27 \pm 0.74	57.32 \pm 8.82*
2-Ketoglutarate	6.75 \pm 0.14	13.67 \pm 1.65*
Malate	13.38 \pm 1.13	46.69 \pm 5.11**
Nicotinate	0.07 \pm 0.02	0.46 \pm 0.03**
Pyruvate	0.64 \pm 0.04	1.68 \pm 0.16**
Shikimate	0.07 \pm 0.01	0.14 \pm 0.04

752

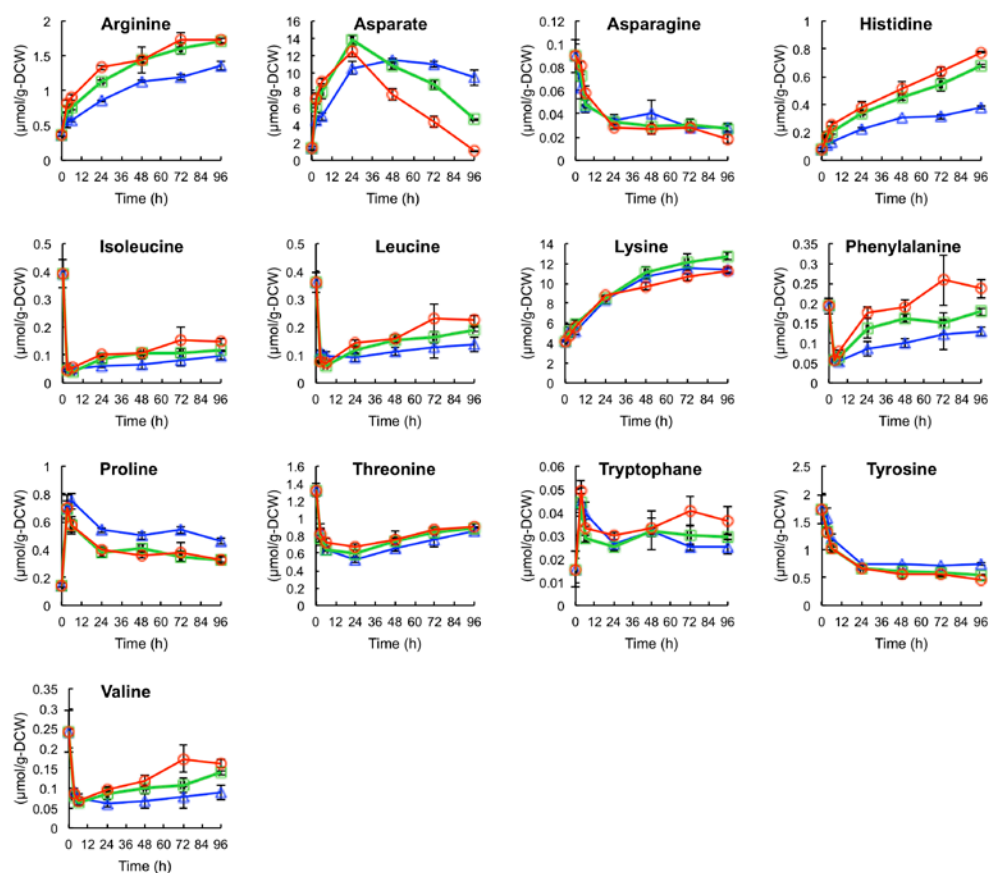
753



754

755 **Fig. S1** Transmission electron micrographs of Ppc-ox cultivated at 30°C and
 756 37°C for 96 h (a). (b) Time course of cell number at 30°C (blue circles), 35°C (purple
 757 circles) and 37°C (red circles). Values represent the average (\pm SD) of three
 758 independent experiments. (c) Decrease in OD₇₅₀ of cells grown at 30°C (blue circles),
 759 35°C (purple circles) and 37°C (red circles). Values represent the average (\pm SD) of
 760 three independent experiments.

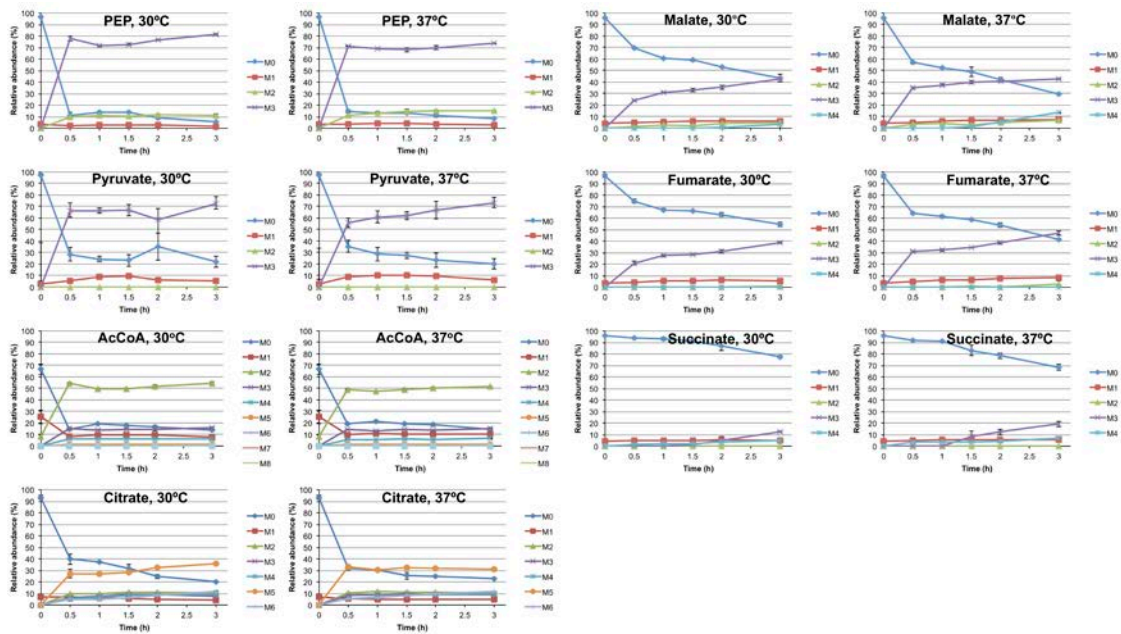
761



762

763 **Fig. S2** Time course of intracellular amino acid pool size in Ppc-ox cultivated at
764 30°C (blue triangles), 35°C (green squares) and 37°C (red circles). Values represent
765 the average (± SD) of three independent experiments.

766



767

768 **Fig. S3** Time-course for mass distribution of metabolites near the pyruvate
 769 branch at 30°C and 37°C. Values are the average (\pm SD) of three independent
 770 experiments. M_i represents the relative isotopomer abundance for each metabolite in
 771 which $i^{13}\text{C}$ atoms are incorporated.